

Lacey, J. H., Leng, M. J., Höbig, N., Reed, J. M., Valero-Garcés, B., and Reicherter, K. 2015. Western Mediterranean climate and environment since Marine Isotope Stage 3: a 50,000-year record from Lake Banyoles, Spain. *Journal of Paleolimnology*, 1-16, doi: 10.1007/s10933-015-9868-9.

This is the author's version of a work that was accepted for publication in *Journal of Paleolimnology* following peer review. Changes may have been made since it was submitted for publication.

The final publication is available at Springer via <http://dx.doi.org/10.1007/s10933-015-9868-9>.

Western Mediterranean climate and environment since Marine Isotope Stage 3: a 50,000-year record from Lake Banyoles, Spain

Jack H. Lacey ^{a,b*}, Melanie J. Leng ^{a,b}, Nicole Höbig ^c, Jane M. Reed ^d, Blas Valero-Garcés ^e, Klaus Reicherter ^c

^a *NERC Isotope Geosciences Facilities, British Geological Survey, Keyworth, Nottingham, NG12 5GG, UK*

^b *Centre for Environmental Geochemistry, School of Geography, University of Nottingham, Nottingham, NG7 2RD, UK*

^c *Institute of Neotectonics and Natural Hazards, RWTH Aachen University, Lochnerstraße 4-20, 52056, Aachen, Germany*

^d *Department of Geography, Environment and Earth Sciences, University of Hull, Hull, HU6 7RX, UK*

^e *Instituto Pirenaico de Ecología, CSIC, Avda Montañana 1005, Apdo 13034, 50080 Zaragoza, Spain*

* *Corresponding author: jackl@bgs.ac.uk*

Keywords: Karstic lakes, Palaeoclimate, Isotopes, Diatoms, Iberian Peninsula, Mediterranean

Abstract

We present new stable isotope ($\delta^{18}\text{O}_{\text{calcite}}$ and $\delta^{13}\text{C}_{\text{calcite}}$) and diatom data from a 67-m sediment core (BAN II) from Lake Banyoles, northeastern Spain. We reassessed the chronology of the sequence by correlating stable isotope data with a shorter U-series-dated record from the lake, confirming a sedimentological offset between the two cores and demonstrating that BAN II spans Marine Isotope Stages (MIS) 3 to 1. Through comparison with previous records, the multi-proxy data are used to improve understanding of palaeolimnological dynamics and, by inference, western Mediterranean climate and environmental change during the past ca. 50,000 years. Three main zones, defined by isotope and diatom data, correspond to the MIS. The basal zone (MIS 3) is characterised by fluctuating $\delta^{18}\text{O}_{\text{calcite}}$ and benthic diatom abundance, indicating a high degree of environmental and climate variability, concomitant with large lake-level changes. During the full glacial (MIS 2), relatively constant $\delta^{18}\text{O}_{\text{calcite}}$ and a poorly preserved planktonic-dominated diatom assemblage suggest stability, and intermittently, unusually high lake level. In MIS 1, $\delta^{18}\text{O}_{\text{calcite}}$ and $\delta^{13}\text{C}_{\text{calcite}}$ initially transition to lower values, recording a pattern of Late Glacial to Holocene change that is similar to other Mediterranean records. This study suggests that Lake Banyoles responds limnologically to changes in the North Atlantic ocean-atmosphere system and provides an important dataset from the Iberian Peninsula, a region in need of longer-term records that can be used to correlate between marine and terrestrial archives, and between the western and eastern Mediterranean.

Introduction

The Iberian Peninsula, located west of the Mediterranean Basin, is a key location for understanding climate connections between the eastern and western Mediterranean (Roberts et al. 2008) and interactions with North Atlantic climate dynamics. The understanding of past climate variability across the peninsula itself has improved considerably over the last two decades, employing a range of proxy methods and sources, including sequences from peatbogs (González-Sampériz et al. 2006), speleothems (Stoll et al. 2013), cave sediment (Fernández et al. 2007), and lacustrine sediment (Reed et al. 2001; Valero-Garcés et al. 2004). Iberian palaeoclimate records show broad similarities, but many do not extend beyond the Holocene and the understanding of pre-Late Glacial climate, in particular, is still limited.

Lake Banyoles, a karst lake located northeast of the Iberian Peninsula (Fig. 1), is a rare Iberian example of a relatively deep, fresh lake with a long sediment record, and is thus an important site for palaeoclimate research in the western Mediterranean. Previous work on Lake Banyoles employed palynological, sedimentological and geochemical techniques for palaeoclimate reconstruction and to improve understanding of the modern physical limnology. In an early palynological study of the lake sediment core, “La Draga” (named after an adjacent Early Neolithic site excavation), Pérez-Obiol and Julià (1994) showed climatic instability during the Glacial, followed by a rapid transition to the Bølling-Allerød interstadial and the Younger Dryas event, suggesting that the lake responds to North Atlantic climate forcing. Valero-Garcés et al. (1998) provided the first palaeohydrological proxy data from sedimentary facies and stable isotope analysis, generating data on regional arid-phase intensity during Heinrich Events (HE; H3-H0) of the last glacial cycle. More recently, Høbig

et al. (2012) used geochemistry and optical methods on core “BAN II” to identify the impact of HE (H5-H0) in the region.

Study site

Lake Banyoles (42°07’N, 02°45’E; 172 m a.s.l.) is located in the Province of Girona, Catalonia, Spain around 25 km from the Mediterranean Sea (Fig. 1). The region has a humid Mediterranean-type climate with an average annual rainfall of 810 mm, measured over the period 2003-2013 at the nearby town of Banyoles (Fig. 2a; <http://www.meteobanyoles.com/>). Minimum precipitation occurs during summer and winter months (July, 37 mm; January, 43 mm), and maximum rainfall is during autumn and spring (October, 116 mm; March, 90 mm). Relative humidity remains fairly stable throughout the year, ranging from 58% (July) to 70% (November). Average monthly temperature ranges from 8°C (January) to 25°C (July), and the annual average temperature is 16°C. The oxygen isotope composition of weighted mean annual precipitation ($\delta^{18}\text{O}_{\text{precipitation}}$) measured at Girona airport (129 m a.s.l., 25 km south of Lake Banyoles) between 2000 and 2006 was -5.7‰ (Fig. 2b; http://www-naweb.iaea.org/napc/ih/IHS_resources_gnip.html). A correction must be applied to incorporate the altitude difference between Girona and Banyoles ($-0.6\text{‰}/100\text{ m}$; Fernández-Chacón et al. 2010); the offset is -0.26‰ for the 43 m altitude increase, which results in a predicted weighted mean annual $\delta^{18}\text{O}_{\text{precipitation}} \approx -5.9\text{‰}$ at Banyoles.

According to the Valero-Garcés et al. (2014) classification of Iberian karst lakes, Banyoles is a hydrologically open system with complex basin morphology and a large watershed. The lake has a maximum length of 2.15 km, a maximum width of 0.78 km and covers 1.12 km^2 (Moreno-Amich and García-Berthou 1989). The average water depth is 14.8

m. The lake can be divided into two (northern and southern) sub-basins separated by a shallow sill, which in turn consist of six isolated, subaqueous karstic sinks, which have a maximum water depth of 46.4 m (Fig. 1; Höbig et al. 2012). Water input to the lake is predominantly through subterranean springs (85%; Serra et al. 2005), where a fault along the eastern shore redirects groundwater flow upwards through the base of the sinks (Moreno-Amich and García-Berthou 1989; Morellón et al. 2014). The underlying confined aquifer is recharged by rainfall from two watersheds located in the Alto-Garroxta mountain range approximately 40 km northwest of Lake Banyoles (Morellón et al. 2014). Five creeks situated on the western shore of the lake supply the remainder of water input (15%; Serra et al. 2005). Groundwater inputs are the dominant influence on modern sedimentation in some of the active sinkholes (Morellón et al. 2014).

The lake sediment is comprised of up to 98% CaCO_3 , including inorganic (endogenic) and biogenic (gastropods, ostracods and charophytes) components, with minor quantities of clays and silt/sand-size particles of mainly quartz and feldspar (Höbig et al. 2012). The lake is therefore characterised as a marl lake, which are typical of Mediterranean karst catchments (Leng and Marshall 2004; Roberts et al. 2008). Average sediment accumulation rate was estimated to be about 1 mm yr^{-1} throughout the La Draga sequence (Pérez-Obiol and Julià 1994), although this value is subject to errors inherent in the previous age model.

Here, we aimed to: 1) improve understanding of the chronology, 2) characterise the nature of palaeohydrological variability for palaeoclimate reconstruction, and 3) constrain periods of lake-level and productivity change in Lake Banyoles. We provide new data from sediment core BAN II, including oxygen ($\delta^{18}\text{O}$) and carbon ($\delta^{13}\text{C}$) isotope data from endogenic calcite, to address (1) and (2) (Leng and Marshall 2004), and diatom data to

provide an indicator of lake-level and productivity change (3) (Currás et al. 2012). Our interpretation is strengthened by multi-proxy comparison with previous work on Lake Banyoles (Pérez-Obiol and Julià 1994; Valero-Garcés et al. 1998; Höbig et al. 2012) and with palaeoclimate reconstructions from the eastern and western Mediterranean, to improve understanding of Late Quaternary variability across this complex region.

Materials and methods

Core recovery and sedimentology

The 67.07-m core, BAN II, was recovered in the early 1990s from the exposed lake bed on the eastern shore of Lake Banyoles (Fig. 1), in 10 cm diameter PVC tubes. The core was collected as 1.5 m-long sections and since collection has been wrapped and stored in darkness at 6°C. In a previous study, the core was dated using Accelerator Mass Spectrometry (AMS ^{14}C) and U-series (U/Th) techniques, and investigated using Multi-Sensor Core Logger, Fourier-Transform Infrared Spectroscopy and X-Ray Fluorescence (XRF) measurements on 366 equidistant samples (Höbig et al. 2012). Here, we incorporate total inorganic carbon (TIC), total organic carbon (TOC), and XRF count data (K, Ca) from this previous work (for analytical methods see Höbig et al. 2012). Ten complex facies were recognised (Höbig et al. 2012), the compositions of which are summarised here to aid multi-proxy interpretation.

The sedimentology of Lake Banyoles reflects several periods of change in the depositional environment (Höbig et al. 2012). The oldest deposits (67.07-41.00 m) are, in general, less variable, with more gradual lithological transition and an intercalated phase of a few-centimetre to decimetre-thick rhythmites (56.00-53.70 m). A major transition occurs at the boundary between facies H and G. The following sediment sequence (41.00-12.00 m) is

highly variable. In the upper sequence (above ~ 12.00 m), the sedimentology indicates subtle changes in the depositional environment.

Facies J (67.07-66.10 m) at the base of the sequence comprises alternating dark- and light-coloured, laminated carbonaceous sediments. There is a gap in core recovery at the transition to facies I (61.20-56.00 m), which shows fining- or coarsening-upward sequences (< 1 m) with embedded clay clasts and intercalated layers of plant fragments, as well as sharp-bounded coarser layers. The overlying sequence (facies E; 56.00-53.70 m) consists mainly of two alternating components (rhythmites), consisting of wavy and/or lenticular, laminated carbonates (clay-silt size) that alternate with coarse (coarse-sand-size) calcified charophyte remains. Facies H is a large and complex unit (53.70-40.00 m), which consists of thick, fining-upward sequences (~ 2 m) dominated at the base by gravel-size *Chara* remains. Further up in the sediment core (facies G; 40.00-33.00 m), thin-bedded silt- and sand-size carbonates were deposited, which have subsequently been buried by about 2 m of facies E-type rhythmites (33.00-31.00 m). The following heterogeneous facies F (31.00-20.00 m) is made of a clayey carbonate matrix, with angular carbonaceous clasts containing abundant charophytes. This is overlain by about 3 m of facies E-type rhythmites (20.00-17.00 m), which have been capped by facies D (17.00-16.00 m). Facies D contains a massive terrestrial freshwater carbonate deposit (travertine, calcareous tufa, and sinter) embedded in lacustrine carbonates. Following this (facies C; 16.00-10.00 m) the depositional environment reverts to lacustrine conditions that have preserved layered carbonate muds with gastropods and plant remains, with some evidence for bioturbation. The latter intensifies in the following facies B (10.00-7.50 m), after which the drill site became sub-aerial, indicated by palustrine carbonates and a peat deposit at the very top of the sequence (3.00-2.00 m) with no core recovery between 7.50 and 3.00 m.

Mineralogy

Mineralogy of the carbonate species was investigated using X-Ray Diffraction (XRD) on a Bruker D8 Advance powder diffractometer equipped with a LynxEye linear position sensitive detector and using $\text{CuK}\alpha$ radiation over the scan range $4\text{-}90^\circ 2\theta$. Phase identification was performed using Bruker DIFFRACplus EVA search/match software, interfaced with the PDF-4+ database from the International Centre for Diffraction Data (ICDD).

Stable isotope analysis of carbonate

Oxygen and carbon isotope analysis of carbonate ($\delta^{18}\text{O}_{\text{calcite}}$ and $\delta^{13}\text{C}_{\text{calcite}}$) was performed at the same subsample intervals as those used in Höbig et al. (2012), comprising 10 cm resolution from the base of the core to the base of the upper peat layer at 2.70 m. For the cross-core correlation, we compared the new isotope data with isotope and palynological data from the La Draga sequence (Pérez-Obiol and Julià 1994; Valero-Garcés et al. 1998).

For isotope analysis the samples were reacted with anhydrous phosphoric acid at a constant 25°C in a vacuum overnight to evolve the CO_2 for analysis. The CO_2 was analysed using a VG Optima dual inlet mass spectrometer. The mineral-gas fractionation factor used for oxygen in calcite was 1.01025, derived from Rosenbaum and Sheppard (1986). $\delta^{18}\text{O}$ and $\delta^{13}\text{C}$ are reported as per mil (‰) deviations of the isotopic ratios ($^{18}\text{O}/^{16}\text{O}$ and $^{13}\text{C}/^{12}\text{C}$) calculated to the Vienna Pee Dee Belemnite (VPDB) scale. Within-run laboratory standards (MCS and CCS) were used, for which analytical reproducibility was $<0.1\text{‰}$ for $\delta^{18}\text{O}_{\text{calcite}}$ and $\delta^{13}\text{C}_{\text{calcite}}$.

A pilot study was carried out using 32 samples selected from throughout the core (with TOC between 0.5% and 7.0%) to assess whether reactive organic matter needed to be removed prior to isotope analysis. One aliquot was analysed using the method described above with no pre-treatment. A second aliquot was disaggregated in 100 ml of 5% sodium hypochlorite for 24 hours to oxidise any reactive organic material, rinsed three times in deionised water, dried at 40°C, ground and the analysis method was applied. The preliminary study showed the two techniques produced similar results (the gradient of treated vs. untreated $\delta^{18}\text{O}$ and $\delta^{13}\text{C} \approx 1$), so processing to remove organic matter was not carried out on the remaining samples.

Diatom analysis

Diatom slides were prepared at a resolution of approximately 0.7-1.0 m intervals (53 subsamples, representing every seventh isotope subsample), using standard techniques (Battarbee et al. 2001). Sediment samples of about 0.1 g were heated in 30% H_2O_2 to oxidise organic material and a few drops of concentrated HCl were added to remove carbonates. The suspension was then washed with deionised water and centrifuged several times to clean and remove clay-size particles. Microscope slides were prepared using Naphrax™. Diatoms were counted at x1000 magnification under oil immersion with a Zeiss Axioscop Plus 2 light microscope. At least 300 valves were counted where diatoms were well preserved, but fewer were enumerated in poorly preserved samples. Diatom identification was based on standard texts, with updated nomenclature (Currás et al. 2012). Ryves' simple F-index (FI), comprising the ratio of pristine to partially dissolved diatom valves (Ryves et al. 2001), was used to summarise preservation status. Diatom results were displayed using Tilia and

TGView, and biostratigraphic zone boundaries were defined using constrained incremental sum of squares (CONISS) cluster analysis (Grimm 2011).

Results

Geochemical and isotope analysis

Calcite is the dominant constituent of the BAN II sediment sequence (Fig. 3; average = $10.1 \pm 1.2\%$ as TIC), which was confirmed by XRD and validated by Scanning Electron Microscopy and Energy-Dispersive X-ray spectroscopy. Total organic carbon (TOC) is generally low, averaging $1.5 \pm 0.8\%$. Three main zones can be defined by eye, based on changes in the isotope data. Zone 3 (67.00-38.50 m) has the lowest average $\delta^{13}\text{C}_{\text{calcite}}$ ($-0.5 \pm 0.8\text{‰}$), intermediate $\delta^{18}\text{O}_{\text{calcite}}$ ($-5.4 \pm 0.4\text{‰}$) and lower, but variable TIC ($9.9 \pm 1.5\%$). Zone 2 (38.50-11.90 m) is defined by higher and less variable $\delta^{18}\text{O}_{\text{calcite}}$ ($-5.1 \pm 0.1\text{‰}$) and TIC ($10.6 \pm 0.5\%$). Zone 1 (11.90-7.70 m) shows high, but variable $\delta^{13}\text{C}_{\text{calcite}}$ ($0.9 \pm 1.0\text{‰}$), the lowest average $\delta^{18}\text{O}_{\text{calcite}}$ ($-6.1 \pm 0.4\text{‰}$) and moderate TIC ($10.2 \pm 0.2\%$). The isotope zones broadly correlate with the facies defined by Höbig et al. (2012), however individual lithological shifts are not generally reflected in the isotope data.

Diatom analysis

A total of 77 diatom taxa were identified, reflecting the diversity of benthic diatom species present at low abundance. Diatom concentration is generally low and most samples show obvious signs of dissolution in the high-alkalinity lake. No diatoms were preserved above 27.4 m depth and slides were uncountable at ~53, 50 and 43 m, and at various levels in the

sequence above 40 m depth. This is reflected in very low FI values, particularly in phases of almost 100% dominance by dissolved *Cyclotella distinguenda* Hustedt, where the FI is consistently <0.2 because the majority of assemblages show strong signs of dissolution.

Six major diatom assemblage zones, DZ1 to DZ6, were defined using CONISS (Fig. 4). Overall, the sequence is dominated by planktonic taxa *Cyclotella distinguenda* Hustedt, an alkaliphilous freshwater diatom that can also tolerate slightly brackish water (Reed 1998), and *Cyclotella ocellata* Pantocsek, a taxon that is probably a species complex, with very broad ecological preferences, but which is common in Mediterranean karst lakes and typically found in shallow to deep, and ultra-oligotrophic to meso-eutrophic water (Reed et al. 2010; Jones et al. 2013). The benthic flora is dominated by freshwater species within the genera *Amphora*, *Diploneis*, *Mastogloia*, *Gomphonema* and *Cymbella*, typical of epiphytic and epipelagic habitats in the littoral zone of Spanish karst lakes (Currás et al. 2012).

DZ1 (60.7-56.7 m)

Planktonic and benthic taxa are present in similar proportions over much of DZ1, with a peak in plankton of >80% in the mid zone corresponding to a minimum in preservation quality. Planktonic *Cyclotella distinguenda* and *C. ocellata* are co-dominant. The benthos is dominated by alkaliphilous *Cymbella leptoceros* (Ehrenberg) Kützing, *Gomphonema angustum* C.A. Agardh non Kützing nec Brébisson fide Grunow in Van Heurck, *Mastogloia lacustris* (Grunow) Grunow in Van Heurck and *Amphora pediculus* (Kützing) Grunow ex A. Schmidt, with facultative planktonic (FP) taxa present at <3% throughout. The FI average for DZ1 is low (0.24).

DZ2 (56.7-51.2 m)

The transition to DZ2 is marked by an increase in the relative abundance of plankton (mainly >85%), with dominance varying between *Cyclotella distinguenda* and *C. ocellata*, and a corresponding decrease in benthic abundance (<30%). Minor peaks in *Achnanthydium minutissimum* (Kützing) Czarnecki and *Sellaphora bacillum* (Ehrenberg) Mann in Round et al. occur at 56.2 m (7.6%) and 52.4 m (11.3%), respectively. The FI average for DZ2 is low (0.18).

DZ3 (51.2-47.3 m)

The relative abundance of benthic taxa drops to <7% in DZ3, with the almost monospecific dominance of *C. distinguenda* (92-100%). *Mastogolia lacustris* and *G. angustum* increase in the centre of the zone (<6%). Preservation is extremely poor, with an FI average of 0.01.

DZ4 (47.3-44.1 m)

The basal sample of DZ4 is characterised by relatively high abundance of benthic taxa, mainly comprising epipelagic *Amphora* spp., a minor increase in FP *Pseudostaurosira brevisstrata* (Grunow in Van Heurck) Williams and Round to 7% and a corresponding decrease in *C. distinguenda* to ~30%. *Cyclotella ocellata* reappears at low abundance (<9%). The remainder of DZ4 is poorly preserved and dominated by *C. distinguenda*, giving an FI average of 0.19.

DZ5 (44.1-41.0 m)

Zone DZ5 is the most distinct of the sequence, being dominated by the FP and benthic taxa, but without a marked shift in the range of taxa. The most notable shift is in FP, with increases in *Staurosira construens* f. *venter* (Ehrenberg) Bukhtiyarova, *P. brevistriata* and *Staurosirella lapponica* (Grunow in Van Heurck) Williams and Round amounting to ~50% abundance at the upper zone boundary, and in *A. pediculus*, which reaches peak abundance of ~30%. Preservation is relatively good, with average FI values of 0.56.

DZ6 (41.0-27.4 m)

Benthic and FP taxa virtually disappear above 40 m depth, in a zone dominated by poorly preserved *C. distinguenda* and a low FI average of 0.07.

Re-assessment of the chronology

The original chronology of BAN II was based on eight Accelerator Mass Spectrometry (AMS ¹⁴C) radiocarbon age estimates and three U/Th radiometric dates (Höbig et al. 2012), with further chronological tie points inferred by cross correlation with a previously U/Th-dated core from Lake Banyoles (Pérez-Obiol and Julià 1994). A horizon of volcanic glass shards, representing a dispersed tephra layer, was geochemically linked to the latest eruptive phase of the Olot volcanic field (ca. 11.5 ka; Höbig et al. 2012). The current age model has been modified to incorporate a radiocarbon reservoir effect (Morellón et al. 2014), and a sedimentological offset between the La Draga and BAN II cores (Fig. 3). The new model shows an improved correlation between radiocarbon and U/Th ages from BAN II, and ages

from the La Draga record (Fig. 5), though age reversals are still prevalent, highlighting the complexity of chronological control.

Radiocarbon dating in karstic lacustrine environments is often subject to lake-water reservoir effects. In Lake Banyoles this generates an error of between +3.0 to +5.5 ka for central lake sediments (Morellón et al. 2014). U-series dating is considered potentially more reliable as there is no reservoir effect and contamination by the secondary migration of U is mitigated by a combination of endogenic calcite deposition with low detrital Th content, high sedimentation rates, and no evidence for sub-aerial exposure (Pérez-Obiol and Julià 1994).

U/Th dates from bulk sediments in the lower section of the BAN II core (below 43.75 m) provide ages between 36 and 52 ka, suggesting they were deposited through MIS 3. This is inferred from a radiocarbon age (taking into account the potential reservoir effect and age limits of the radiocarbon technique) at 61.06 m of ca. 48 ka, and also suggested by pollen data, wherein the percentage of mesophilous taxa is higher at the base of the La Draga core (Pérez-Obiol and Julià 1994). The subsequent AMS ^{14}C ages show a linear progression through the core and, although offset, display a similar trend to U/Th ages. This suggests a relatively stable sediment accumulation rate over the past ca. 50 ka, however ^{14}C ages still offer poor overall chronological control in the BAN II sequence. The new isotope data presented here allow for more precise correlation with the previous core from Lake Banyoles, wherein maximum values of both $\delta^{18}\text{O}$ and $\delta^{13}\text{C}$ occurred at 6.10 m during the Younger Dryas in La Draga (Valero-Garcés et al. 1998). These peaks can be correlated to those at 11.90 m in BAN II, which suggests a potential 5.80 m offset between the two cores. Sediment deposition during the Holocene is indicated by a radiocarbon date taken from a peat layer (terrestrial, no reservoir effect) at 2.8 m (5367 ± 66 cal yr BP), and by increasing TOC through

Zone I. Our results therefore support the previous argument that core BAN II covers MIS 3-1 (Höbig et al. 2012), but the age model is now strengthened by isotope correlation between cores. The zones (3-1) defined by isotope data broadly correlate to MIS 3-1 based on the chronological data available.

Discussion

Modern lake-water isotope composition and controls

Lake Banyoles is fed by a large karst aquifer system, formed in Palaeogene limestone and gypsum, with an estimated hydrological throughput of about 1 hectometre³ per day (Pérez-Obiol and Julià 1994). Although our modern water isotope dataset is small, it can be inferred from BAN II data that consistently low $\delta^{18}\text{O}_{\text{calcite}}$ with relatively minimal down-core variability ($-5.4 \pm 0.4\text{‰}$, 1σ , $n = 334$) reflects a hydrologically open system with a short residence time, in which the isotope composition of aquifer and lake water are similar (Valero-Garcés et al. 2014). The modern isotope composition of lake water ($\delta^{18}\text{O}_{\text{lakewater}}$) from Lake Banyoles was measured in 2011 and gave a mean $\delta^{18}\text{O}_{\text{lakewater}} = -5.4 \pm 0.5\text{‰}$ (1σ , $n = 11$; B. Valero-Garcés, unpublished data), which is generally consistent with the mean annual rainfall isotope composition ($\approx -5.9\text{‰}$; Fig. 2). This suggests that, in general, $\delta^{18}\text{O}_{\text{lakewater}}$ is not affected by evaporative processes, which is corroborated by low lake-water electrical conductivity (Moreno-Amich et al. 2006), indicating a water column that is deficient in total dissolved solids (Rosqvist et al. 2007). Hence, for understanding past lake water balance, $\delta^{18}\text{O}_{\text{lakewater}}$ variations are thought primarily to reflect changes in $\delta^{18}\text{O}_{\text{precipitation}}$ (i.e. temperature, source, continentality, altitude, amount, seasonality), rather than internal-lake processes, such as evaporation (Leng and Marshall 2004).

Temperature and precipitation patterns in the North Atlantic region are dominated by the North Atlantic Oscillation (NAO; Sánchez Goñi et al. 2002). Complex orography and other local geographical factors moderate the influence of North Atlantic atmospheric dynamics in some regions (Martin-Vide and Lopez-Bustins 2006), however, and create strong regional differences in the seasonal timing of maximum precipitation. The majority of water delivered to the Iberian Peninsula originates from two sources: the Atlantic Ocean and Mediterranean Sea, which produce a distinct source effect on $\delta^{18}\text{O}_{\text{precipitation}}$ received at Banyoles (Moreno et al. 2014). The importance of rainfall from each individual source varies both regionally and seasonally (Gimeno et al. 2010; Moreno et al. 2014), and the extent of influence can be potentially identified using the deuterium excess (*d*-excess; $\delta\text{D} - 8\delta^{18}\text{O}$) of meteoric water (Fernández-Chacón et al. 2010).

Following evaporation from an ocean source, *d*-excess does not significantly change during subsequent modification within an evolving air mass, as typically $\delta^{18}\text{O}$ and δD vary proportionately (Sharp 2007). The global average *d*-excess is 10‰ (Dansgaard 1964) and varies spatially because of differences in humidity, wind speed and sea surface temperatures, whereby higher humidity results in lower *d*-excess values (Clark and Fritz 1997). Furthermore, seasonal variation is induced by reduced relative humidity over the oceans during winter months, and kinetic effects in arid regions under intense evaporation lead to greatly enhanced *d*-excess values (Sharp 2007). In the western Mediterranean Basin *d*-excess is reported as 13.7‰ (Celle-jeanton et al. 2001), intermediate between the global average and that for the eastern Mediterranean (20‰; Dotsika et al. 2010). The isotope composition of precipitation falling at Girona (25 km south of Lake Banyoles) was measured between 2000 and 2006 (http://www-naweb.iaea.org/naweb/ih/IHS_resources_gnip.html), from which

monthly values for d -excess were calculated (Fig. 6). The majority of average values are either below or approaching the global average d -excess ($7.4 \pm 3.5\%$, 1σ), and a lesser percentage of individual monthly values are found to exhibit higher d -excess. The higher values may well be associated with convective systems that originate from the Mediterranean (Moreno et al. 2014), however in general d -excess values are below or equal to that of the global average. This may suggest that most of the water delivered to the Banyoles area, during the periods of peak rainfall at least, is derived principally from an Atlantic source.

Oxygen isotope composition of calcite from Lake Banyoles

The oxygen isotope composition of the water in Lake Banyoles ($\delta^{18}\text{O}_{\text{lakewater}}$) is assumed to be captured in $\delta^{18}\text{O}_{\text{calcite}}$ produced in the surface waters at a given temperature, and $\delta^{18}\text{O}_{\text{lakewater}}$ will dominantly reflect some aspect of $\delta^{18}\text{O}_{\text{precipitation}}$ (Leng and Marshall 2004). Variations in $\delta^{18}\text{O}_{\text{precipitation}}$ are regulated by a number of factors including the condensation temperature, source changes, evaporation, ‘amount’ effects and seasonality (Leng and Marshall 2004). Assuming the calcite was precipitated in equilibrium, the oxygen isotope composition of mean annual precipitation correlates to temperature change in the northern hemisphere by approximately $+0.6\%/^{\circ}\text{C}$ (Dansgaard 1964), which is opposed by a mineral-water isotope fractionation of $-0.24\%/^{\circ}\text{C}$. Therefore, $\delta^{18}\text{O}_{\text{calcite}}$ correlates to temperature with a gradient of roughly $+0.36\%/^{\circ}\text{C}$ (Leng and Marshall 2004). This suggests that if temperature is directly driving changes in $\delta^{18}\text{O}_{\text{calcite}}$ (i.e. no change in source of precipitation), values should be lower during glacial times because of the colder climate, which is true for records from the Alpine region and central Europe (Grafenstein et al. 1999; Schwander et al. 2000). However, in Lake Banyoles this is not the case as there is a shift from higher $\delta^{18}\text{O}_{\text{calcite}}$ in Zone 2 (MIS 2) to lower $\delta^{18}\text{O}_{\text{calcite}}$ in Zones 1 and 3 (MIS 1 and 3). This change to generally lower $\delta^{18}\text{O}$

values during wetter (and warmer) phases is seen across the majority of Mediterranean lake interglacial/interstadial records. On a glacial-interglacial timescale, temperature is considered a secondary driver of Mediterranean isotope composition compared to water balance, which is lower during cold, but highly arid glacial phases (Roberts et al. 2008).

The configuration of long-term variations in $\delta^{18}\text{O}_{\text{calcite}}$ is similar to that recorded in Greenland ice cores (NGRIP Members 2004), by planktic foraminifera from the western Portuguese margin (de Abreu et al. 2003), the Alborán Sea (Cacho et al. 1999), the Ionian Sea (Allen et al. 1999) and by speleothems from Israel (Bar-Matthews et al. 1999) (Fig. 7). Congruence with these records means that $\delta^{18}\text{O}_{\text{calcite}}$ could be primarily driven by changes linked to the Northern Hemisphere ocean-atmosphere system during the last glacial-interglacial cycle, and suggests that a close association exists between North Atlantic and western-eastern Mediterranean climates. Furthermore, this also suggests that North Atlantic climate dynamics are most likely the primary control on the isotope composition of precipitation at Lake Banyoles, with Mediterranean sources of precipitation only of minor, secondary importance.

Carbon isotope composition of calcite from Lake Banyoles

We assume BAN II carbonates capture the $\delta^{13}\text{C}$ of the lake water in which they precipitated (Leng and Marshall 2004), which will generally reflect the isotope composition of total dissolved inorganic carbon ($\delta^{13}\text{C}_{\text{TDIC}}$). This can be approximated to the isotope composition of aqueous HCO_3^- for most lakes. As only a small fractionation occurs during precipitation, $\delta^{13}\text{C}_{\text{calcite}}$ can indicate past variations in $\delta^{13}\text{C}_{\text{TDIC}}$ and carbon cycle transitions. In lakes, $\delta^{13}\text{C}_{\text{TDIC}}$ is mainly influenced by the isotope composition of inflowing waters, and by

subsequent modification through kinetic processes (Leng and Marshall 2004). Groundwater inflows typically have relatively low $\delta^{13}\text{C}_{\text{TDIC}}$ because of the incorporation of isotopically light carbon liberated from the decay of organic matter in soils, which has average $\delta^{13}\text{C} = -30$ to -16‰ , for a combination of C3 ($\delta^{13}\text{C} -32$ to -20‰) and C4 ($\delta^{13}\text{C} -17$ to -9‰) plants (Leng et al. 1999). Following decay, light carbon (CO_2) enters groundwater by dissolution, is hydrated to produce carbonic acid and dissociates to predominantly form bicarbonate (at neutral pH), which has a fractionation factor of approximately $+10\text{‰}$ when in equilibrium with CO_2 (Mook et al. 1974). Thus, $\delta^{13}\text{C}_{\text{TDIC}}$ derived solely from C3 soil- CO_2 is predicted to have $\delta^{13}\text{C}$ between -22 to -10‰ , and C4 soil- CO_2 between -7 to $+1\text{‰}$. Catchment vegetation is known to have comprised varying percentages of both arboreal and non-arboreal taxa through time (Pérez-Obiol and Julià 1994). Therefore, the estimated values for $\delta^{13}\text{C}_{\text{TDIC}}$ are isotopically lower than both the Banyoles modern surface waters ($\delta^{13}\text{C}_{\text{DIC}} = -3.3\text{‰}$, measured in 2011; B. Valero-Garcés, unpublished data) and BAN II core data ($\delta^{13}\text{C}_{\text{calcite}}$ range = -3.4‰ to $+2.9\text{‰}$), suggesting that organic-derived soil- CO_2 is potentially a component of $\delta^{13}\text{C}_{\text{TDIC}}$, although in addition there must be an isotopically heavier $\delta^{13}\text{C}$ source.

It is unlikely that high $\delta^{13}\text{C}_{\text{calcite}}$ is the product of equilibration with atmospheric CO_2 , which can yield $\delta^{13}\text{C}$ in excess of $+3\text{‰}$ (Leng and Marshall 2004), a consequence of the short lake-water residence time. As the predominant water input to Lake Banyoles is through karst aquifers, it is likely that the majority of ^{13}C -enriched HCO_3^- is derived through the dissolution of aquifer carbonates, as geological sources of carbonate generally have high $\delta^{13}\text{C}$ values, between -3‰ to $+3\text{‰}$ (Leng et al. 1999). In addition, aquatic productivity may act to raise $\delta^{13}\text{C}_{\text{TDIC}}$, as during photosynthesis the preferential uptake of ^{12}C can leave TDIC isotopically heavy. In Banyoles this process may take place during restricted intervals (e.g. around 44 m),

however commensurate increases in TOC would also be expected, which generally are not observed.

Excursions to lower $\delta^{13}\text{C}_{\text{calcite}}$ could be ascribed to the release of ^{12}C as a product of degradation processes following organic carbon oxidation in bottom waters, which would also likely result in low values of TOC. In Lake Banyoles this does not appear to be the case, as TOC is generally low throughout the core and shows no correlation with $\delta^{13}\text{C}_{\text{calcite}}$ ($r = -0.18$). Transitions to lower $\delta^{13}\text{C}_{\text{calcite}}$ are more probably driven by enhanced delivery of ^{12}C during times of soil development within the catchment, and associated with an increased contribution from isotopically light carbon derived from terrestrial C3 plants during warmer periods, for example as seen in the early Holocene (Fig. 3; Valero-Garcés et al. 1998).

Variations in $\delta^{13}\text{C}_{\text{calcite}}$ are thought to be mainly a product of the balance between the contribution from the bicarbonate ion, in addition to the concentration and constitution of soil CO_2 . During times of enhanced soil development within the catchment (e.g. within the Holocene), $\delta^{13}\text{C}_{\text{calcite}}$ is expected to be lower, as more isotopically light carbon is assumed to be incorporated into TDIC. In times of restricted soil development, commensurate with increased percentages of steppic C4 taxa, $\delta^{13}\text{C}_{\text{calcite}}$ will be higher.

Isotope covariance and facies variability

Carbonates produced in open lakes typically do not show covariance between $\delta^{18}\text{O}$ and $\delta^{13}\text{C}$ (Talbot 1990), whereas in closed systems the degree of covariance depends on several factors such as atmospheric exchange, evaporation rates, and productivity (Li and Ku 1997). Lake Banyoles displays no covariance between $\delta^{18}\text{O}_{\text{calcite}}$ and $\delta^{13}\text{C}_{\text{calcite}}$ over the whole core ($r =$

0.10), which most likely reflects its short lake-water residence time as a throughflow-dominated system. Covariance increases during certain periods when constrained time zones are considered, specifically during the Holocene ($r = 0.75$) and the $\delta^{18}\text{O}_{\text{calcite}}$ maximum toward the upper boundary of Zone III ($r = 0.88$). However, increased covariance does not necessarily relate to hydrological closure as, at least for the Holocene, there is a general transition to lower $\delta^{18}\text{O}_{\text{calcite}}$ and $\delta^{13}\text{C}_{\text{calcite}}$, most likely caused by enhanced freshwater input and the development of catchment soils. Furthermore, approaching the upper boundary of Zone III, there is a distinct parallel excursion to higher isotope values that occurs alongside a peak in TOC and TIC after 44 m. Lower lake level is indicated at that time by the preservation of benthic diatom taxa in DZ4, which suggests rapid sedimentation in a littoral zone with aquatic plants (increased TOC) during a shallow-water phase. High TIC and TOC indicate enhanced productivity at that time, which may be associated with the preferential removal of ^{12}C in the epilimnion driving increased $\delta^{13}\text{C}_{\text{calcite}}$. High $\delta^{18}\text{O}_{\text{calcite}}$ was probably a function of regional climate, related to seasonal temperature changes leading to higher $\delta^{18}\text{O}$ summer precipitation and increased aridity (Leng et al. 1999).

In general, there is little correlation between $\delta^{18}\text{O}_{\text{calcite}}$ and facies variability in BAN II, suggesting that isotope values are somewhat independent of changes in lake level. This perhaps indicates that during times of reduced lake level, assumed to be related to coarser-grained facies in BAN II (Höbig et al. 2012) and regional aridity, lake water is hydrologically buffered against the effects of evaporation and kinetic fractionation. Höbig et al. (2012) suggested that four horizons have characteristics potentially attributed to slump-related processes (Fig. 3). The tilted nature of the basal horizon (67.07-66.10 m; facies J) suggests these sediments are indeed slumped, therefore precluding robust environmental reconstruction. However, the overlying horizons do not show the same physical appearance

and appear to be undisturbed, which suggests stratigraphic variability could potentially be related to lake-level changes.

Lake Banyoles climate and hydrology: MIS 3-1

During the last glacial period there was considerable climatic variability across the North Atlantic (Dansgaard et al. 1993), attributed to changes in thermohaline circulation and subsequent modification of ocean heat transport (Clark et al. 2002). Mediterranean marine and lacustrine records suggest that the region closely reflected the North Atlantic ocean-atmosphere system (Allen et al. 1999) and that at a millennial scale, climatic fluctuations showed a Dansgaard–Oeschger (D-O) pattern of variability (Cacho et al. 1999). During cold D-O phases, enhanced northern hemisphere atmospheric circulation is suggested by increased Saharan dust transport and incorporation in western Mediterranean Sea sediments (Moreno 2002), causing higher-intensity wind systems over the Iberian Peninsula, predominantly from the west and northwest (Vegas et al. 2010). Oscillations in atmospheric moisture content during cold and arid stadial and mild and wet interstadial periods are inferred from the Alborán Sea, which shows an alternating steppe to deciduous-evergreen pollen assemblage (Sánchez Goñi et al. 2002). This record also suggests that an extreme climate state existed during Heinrich Events (HE), which are characterised by aridity and colder conditions in the Mediterranean (Sánchez Goñi et al. 2002). Central Spain is thought to have been colder and experienced enhanced aridity during these cold events, with widespread growth of herbaceous plant steppe taxa, suggesting a near-instantaneous transfer of climate state between the northern Atlantic to the Iberian Peninsula (Vegas et al. 2010).

In Lake Banyoles, millennial-scale $\delta^{18}\text{O}_{\text{calcite}}$ and $\delta^{13}\text{C}_{\text{calcite}}$ shifts through MIS 3 (Fig. 3) may be analogous to enhanced variability observed across the North Atlantic and western Mediterranean (Fig. 7; Cacho et al. 1999; de Abreu et al. 2003). Although the chronology could be better constrained, a response to abrupt HE has been suggested from previous reconstructions from the lake (Valero-Garcés et al. 1998; Höbig et al. 2012) and in the surrounding region (González-Sampériz et al. 2006). However, there is evidence neither for cold or arid rapid-climate-change events in $\delta^{18}\text{O}_{\text{calcite}}$ or $\delta^{13}\text{C}_{\text{calcite}}$ data (Fig. 3), which may be a consequence of the relative unimportance of evaporative effects on the lake water and the short residence time. Other proxies (e.g. K/Ca, Fig. 3) appear to be more sensitive to increased aridity and reflect local environmental conditions more closely. The abundance of *C. ocellata* in mid-MIS 3 (DZ1 to DZ2) may indicate higher productivity and, by inference, temperature, an association reported from other Mediterranean lakes, such as Lake Ohrid (Reed et al. 2010). The return to very poor diatom preservation and dominance by *C. distinguenda* above ~51 m depth correlates with a lithological shift to finer-grain sediment, indicative of lake-level increase corresponding to a reduction in TOC, which suggests low, temperature-induced productivity associated with reduced evaporation, but without a strong associated isotopic signal. Towards the end of MIS 3, diatoms provide strong evidence for a shallowing trend in the proportion of benthic and FP taxa, which correlates with increased TOC and higher-quality preservation in the more organic littoral zones of Banyoles. The concomitant covariant excursion in $\delta^{18}\text{O}_{\text{calcite}}$ and $\delta^{13}\text{C}_{\text{calcite}}$ to higher values suggests this is a response to increasing aridity, and most likely related to the lake volume change indicated by the transition to a benthic-dominated diatom assemblage.

Through MIS 2 and surrounding the last glacial maximum, proxies from Lake Banyoles (notably TIC and $\delta^{18}\text{O}_{\text{calcite}}$) become less variable and the sedimentology is

primarily characterised by fine-grained, clay-rich facies (Valero-Garcés et al. 1998; Höbig et al. 2012). Benthic and FP diatom taxa are essentially absent, and poorly preserved *C. distinguenda* becomes dominant, suggesting a low-productivity ‘deep’ lake, which is also suggested by low- $\delta^{13}\text{C}_{\text{calcite}}$, representing a decrease in productivity-driven ^{13}C enrichment. Thus, diatom data and sedimentology provide strong proxy evidence for increased lake level during MIS 2. This must be a function mainly of low evaporative concentration with reduced temperature, as the presence of *Artemisia* steppe vegetation in the catchment (Fig. 3; Pérez-Obiol and Julià 1994) provides strong proxy evidence for aridity. There is also ample pollen-based evidence that MIS 2 was extremely arid across the region as a whole (Roucoux et al. 2005). High lake levels during glacial times are also found in some Mediterranean records (Kolodny et al. 2005), but most shallow alkaline lakes are at a low level (Jones et al. 2013). Higher lake levels could be caused by a combination of lower temperatures, leading to less evaporative concentration, and a reduction in catchment vegetation cover, resulting in lower rates of evapotranspiration, which encourages aquifer throughflow and deeper lacustrine conditions.

The Late Glacial to Holocene sequence of climate and environmental change from Lake Banyoles is consistent with that of the previous studies from the lake (Valero-Garcés et al. 1998) and of other Mediterranean lacustrine records (Roberts et al. 2008). There is a shift to higher $\delta^{18}\text{O}_{\text{calcite}}$, reaching a maximum at 11.9 m in the core, which can be correlated to a similar rise in the previous isotope record at 6.1 m and a significant rise in *Artemisia* and decrease in *Pinus*, signifying the re-expansion of steppe conditions (Fig. 3; Pérez-Obiol and Julià 1994; Valero-Garcés et al. 1998). The interval, dated to 12 ka (Pérez-Obiol and Julià 1994), therefore likely corresponds to the Younger Dryas event and can be compared to similar excursions in both western and eastern Mediterranean records (Fig. 7). The absence of

diatoms during the Holocene is consistent with their poor preservation in lake-centre sediment during maximum lake-level phases, caused by dissolution in the water column. One of the most distinct $\delta^{18}\text{O}_{\text{calcite}}$ excursions in Lake Banyoles is through the Late Glacial to Holocene transition, with a maximum change of -2‰ (-4.7‰ at 11.9 m, -6.7‰ at 8.5 m). A shift to lower $\delta^{18}\text{O}_{\text{calcite}}$ is a prominent feature that is common across most Mediterranean lakes during that time (Roberts et al. 2008), and is comparable in magnitude to the changes in the composition of western Iberian margin and Alborán Sea planktic foraminifera (Cacho et al. 1999; de Abreu et al. 2003). The subsequent excursion to higher $\delta^{18}\text{O}_{\text{calcite}}$ at 9.3 m may correspond to the 8.2 ka event, which is constrained by a U/Th date at 10.8 m (9.7 ka), assuming a 5.8-m offset between the BAN II and La Draga cores.

Conclusions

We presented new stable isotope data ($\delta^{18}\text{O}_{\text{calcite}}$ and $\delta^{13}\text{C}_{\text{calcite}}$) from Lake Banyoles, which were combined with previous data (TIC, TOC, K/Ca) from the same core (Höbig et al. 2012) and compared to a shorter core from the lake that provided isotope and pollen records (Pérez-Obiol and Julià 1994; Valero-Garcés et al. 1998). The current age model (Höbig et al. 2012) has been modified, but we agree the core likely spans MIS 3-1, based on U/Th ages and correlation between the two sets of isotope data. U/Th ages provide the best potential age control for extended sequences recovered from Lake Banyoles, given the observed radiocarbon offset. Lake Banyoles $\delta^{18}\text{O}_{\text{calcite}}$ appears to primarily reflect a distinct source effect on $\delta^{18}\text{O}_{\text{precipitation}}$ and glacial-interglacial changes in the composition of marine source waters. Investigation of local precipitation data shows overall low d -excess and suggests that the majority of rainfall received by Lake Banyoles probably derives from Atlantic fronts rather than Mediterranean origin. The sequence from Lake Banyoles has been divided into three main zones that broadly correlate to MIS 3-1 based on the chronological information

available, changes in the isotope composition of the sediments, and diatom assemblage data. Zone 3 shows a greater number of larger-amplitude excursions in $\delta^{18}\text{O}_{\text{calcite}}$, and $\delta^{13}\text{C}_{\text{calcite}}$, which are coincident with considerable millennial-scale climate fluctuations across the North Atlantic and surrounding regions. Enhanced variability in TOC and the presence of benthic diatoms suggests MIS 3 was characterised by substantial lake level shifts and associated productivity changes. A generally more stable climate can be inferred for Zone 2, with $\delta^{18}\text{O}_{\text{calcite}}$ being higher and, along with TIC and TOC, more consistent. There may have been a high-lake-level phase at that time, suggested by a decrease in diatom preservation and a sedimentology indicative of deeper water. The transition between Zone 2 and Zone 1 shows a distinct change to lower $\delta^{18}\text{O}_{\text{calcite}}$, a pattern that is common amongst Mediterranean lake records. This study provides an important extended multi-proxy continuous record for the Iberian Peninsula, and offers a new Late Quaternary palaeoclimate archive to correlate between terrestrial and marine records from both the western and eastern Mediterranean, thus reinforcing hemispheric teleconnections.

Acknowledgements

This paper contributes to the CRC 806 (University of Cologne) – Our Way to Europe. The paper forms part of the PhD research of JHL funded by the British Geological Survey University Funding Initiative (BUFI) and also the PhD of NH at RWTH Aachen University. Thanks go to Andrea Snelling (NIGL) for assistance with the isotope work and Cheryl Haidon (University of Leicester) for providing mineralogy data.

References

Allen JRM, Brandt U, Brauer A, Hubberten HW, Huntley B, Keller J, Kraml M, Mackensen A, Mingram J, Negendank JFW, Nowaczyk NR, Oberhänsli H, Watts WA, Wulf S, Zolitschka B. (1999) Rapid environmental changes in southern Europe during the last glacial period. *Nature* 400:740-743

Bar-Matthews M, Ayalon A, Kaufman A, Wasserburg GJ. (1999) The Eastern Mediterranean paleoclimate as a reflection of regional events: Soreq cave, Israel. *Earth Planet Sc Lett* 166:85-95

Battarbee RW, Jones VJ, Flower RJ, Cameron NG, Bennion H. (2001) Diatoms. In: Smol JP, Birks HJB, Last WM (eds), *Tracking Environmental Change using Lake Sediments*. Kluwer Academic Publishers, Dordrecht, pp 155-202

Blockley SPE, Lane CS, Hardiman M, Rasmussen SO, Seierstad IK, Steffensen JP, Svensson A, Lotter AF, Turney CSM, Bronk Ramsey C. (2012) Synchronisation of palaeoenvironmental records over the last 60,000 years, and an extended INTIMATE event stratigraphy to 48,000 b2k. *Quaternary Sci Rev* 36:2-10

Cacho I, Grimalt JO, Pelejero C, Canals M, Sierro FJ, Flores JA, Shackleton N. (1999) Dansgaard-Oeschger and Heinrich event imprints in Alborán Sea paleotemperatures. *Paleoceanography* 14:698-705

Celle-Jeanton H, Gonfiantini R, Travi Y, Sol B. (2004) Oxygen-18 variations of rainwater during precipitation: application of the Rayleigh model to selected rainfalls in Southern France. *J Hydrol* 289:165-177

Celle-Jeanton H, Travi Y, Blavoux B. (2001) Isotopic typology of the precipitation in the Western Mediterranean Region at three different time scales. *Geophys Res Lett* 28:1215-1218

Clark ID, Fritz P. (1997) *Environmental Isotopes in Hydrogeology*. CRC Press/Lewis Publishers, Boca Raton, Florida

Clark PU, Pisias NG, Stocker TF, Weaver AJ. (2002) The role of the thermohaline circulation in abrupt climate change. *Nature* 415:863-869

Craig H. (1961) Isotopic Variations in Meteoric Waters. *Science* 133:1702-1703

Currás A, Zamora L, Reed JM, García-Soto E, Ferrero S, Armengol X, Mezquita-Joanes F, Marqués MA, Riera S, Julià R. (2012) Climate change and human impact in central Spain during Roman times: High-resolution multi-proxy analysis of a tufa lake record (Somolinos, 1280m asl). *Catena* 89:31-53

Dansgaard W. (1964) Stable isotopes in precipitation. *Tellus* 16:436-468

Dansgaard W, Johnsen SJ, Clausen HB, Dahl-Jensen D, Gundestrup NS, Hammer CU, Hvidberg CS, Steffensen JP, Sveinbjörnsdóttir AE, Jouzel J, Bond G. (1993) Evidence for general instability of past climate from a 250-kyr ice-core record. *Nature* 364:218-220

de Abreu L, Shackleton NJ, Schönfeld J, Hall M, Chapman M. (2003) Millennial-scale oceanic climate variability off the Western Iberian margin during the last two glacial periods. *Mar Geol* 196:1-20

Dotsika E, Lykoudis S, Poutoukis D. (2010) Spatial distribution of the isotopic composition of precipitation and spring water in Greece. *Global Planet Change* 71:141-149

Fernández-Chacón F, Benavente J, Rubio-Campos JC, Kohfahl C, Jiménez J, Meyer H, Hubberten H, Pekdeger A. (2010) Isotopic composition ($\delta^{18}\text{O}$ and δD) of precipitation and groundwater in a semi-arid, mountainous area (Guadiana Menor basin, Southeast Spain). *Hydrol Process* 24:1343-1356

Fernández S, Fuentes N, Carrión JS, González-Sampériz P, Montoya E, Gil G, Vega-Toscano G, Riquelme JA. (2007) The Holocene and Upper Pleistocene pollen sequence of Carihuela Cave, southern Spain. *Geobios* 40:75-90

- Gimeno L, Nieto R, Trigo RM, Vicente-Serrano SM, López-Moreno JI. (2010) Where Does the Iberian Peninsula Moisture Come From? An Answer Based on a Lagrangian Approach. *J Hydrometeorol* 11:421-436
- González-Sampériz P, Valero-Garcés BL, Moreno A, Jalut G, García-Ruiz JM, Martí-Bono C, Delgado-Huertas A, Navas A, Otto T, Dedoubat JJ. (2006) Climate variability in the Spanish Pyrenees during the last 30,000 yr revealed by the El Portalet sequence. *Quaternary Res* 66:38-52
- Grafenstein Uv, Erlenkeuser H, Brauer A, Jouzel J, Johnsen SJ. (1999) A Mid-European Decadal Isotope-Climature Record from 15,500 to 5000 Years B.P. *Science* 284:1654-1657.
- Grimm EC. (2011) *Tilia and Tilia-Graph*. Illinois State Museum, Springfield, USA
- Höbig N, Weber ME, Kehl M, Weniger G-C, Julià R, Melles M, Fülöp R-H, Vogel H, Reicherter K. (2012) Lake Banyoles (northeastern Spain): A Last Glacial to Holocene multi-proxy study with regard to environmental variability and human occupation. *Quatern Int* 274:205-218
- Jones TD, Lawson IT, Reed JM, Wilson GP, Leng MJ, Gierga M, Bernasconi SM, Smittenberg RH, Hajdas I, Bryant CL, Tzedakis PC. (2013) Diatom-inferred Late Pleistocene and Holocene palaeolimnological changes in the Ioannina basin, northwest Greece. *J Paleolimnol* 49:185-204
- Kolodny Y, Stein M, Machlus M. (2005) Sea-rain-lake relation in the Last Glacial East Mediterranean revealed by $\delta^{18}\text{O}$ - $\delta^{13}\text{C}$ in Lake Lisan aragonites. *Geochim Cosmochim Acta* 69:4045-4060
- Leng MJ, Marshall JD. (2004) Palaeoclimate interpretation of stable isotope data from lake sediment archives. *Quaternary Sci Rev* 23:811-831

Leng MJ, Roberts N, Reed JM, Sloane HJ. (1999) Late Quaternary palaeohydrology of the Konya Basin, Turkey, based on isotope studies of modern hydrology and lacustrine carbonates. *J Paleolimnol* 22:187-204

Li HC, Ku TL. (1997) $\delta^{13}\text{C}$ - $\delta^{18}\text{O}$ covariance as a paleohydrological indicator for closed-basin lakes. *Palaeogeogr Palaeoclimatol* 133:69-80

Martin-Vide J, Lopez-Bustins J-A. (2006) The Western Mediterranean Oscillation and rainfall in the Iberian Peninsula. *Int J Climatol* 26:1455-1475

Mook WG, Bommerson JC, Staverman WH. (1974) Carbon isotope fractionation between dissolved bicarbonate and gaseous carbon dioxide. *Earth Planet Sc Lett* 22:169-176

Morellón M, Anselmetti FS, Valero-Garcés B, Giralt S, Ariztegui D, Sáez A, Mata MP, Barreiro-Lostrés F, Rico M, Moreno A. (2014) The influence of subaquatic springs in lacustrine sedimentation: Origin and paleoenvironmental significance of homogenites in karstic Lake Banyoles (NE Spain). *Sediment Geol* 311:96-111

Moreno-Amich R, García-Berthou E. (1989) A new bathymetric map based on echosounding and morphometrical characterization of the Lake of Banyoles (NE-Spain). *Hydrobiologia* 185:83-90

Moreno-Amich R, Pou-Rovira Q, Vila-Gispert A, Zamora L, García-Berthou E. (2006) Fish ecology in Lake Banyoles (NE Spain): A tribute to Ramon Margalef. *Limnetica* 25:321-334

Moreno A. (2002) Saharan Dust Transport and High-Latitude Glacial Climatic Variability: The Alborán Sea Record. *Quaternary Res* 58:318-328

Moreno A, Sancho C, Bartolomé M, Oliva-Urcia B, Delgado-Huertas A, Estrela MJ, Corell D, López-Moreno JI, Cacho I. (2014) Climate controls on rainfall isotopes and their effects on cave drip water and speleothem growth: the case of Molinos cave (Teruel, NE Spain). *Clim Dynam* 43:221-241

NGRIP Members. (2004) High-resolution record of Northern Hemisphere climate extending into the last interglacial period. *Nature* 431:147-151

Pérez-Obiol R, Julià R. (1994) Climatic Change on the Iberian Peninsula Recorded in a 30,000-Yr Pollen Record from Lake Banyoles. *Quaternary Res* 41:91-98

Reed JM. (1998) Diatom preservation in the recent sediment record of Spanish saline lakes: Implications for palaeoclimate study. *J Paleolimnol* 19:129-137

Reed JM, Cvetkoska A, Levkov Z, Vogel H, Wagner B. (2010) The last glacial-interglacial cycle in Lake Ohrid (Macedonia/Albania): testing diatom response to climate. *Biogeosciences* 7:3083-3094

Reed JM, Stevenson AC, Juggins S. (2001) A multi-proxy record of Holocene climatic change in southwestern Spain: The Laguna de Medina, Cádiz. *Holocene* 11:707-719

Roberts N, Jones MD, Benkaddour A, Eastwood WJ, Filippi ML, Frogley MR, Lamb HF, Leng MJ, Reed JM, Stein M, Stevens L, Valero-Garcés B, Zanchetta G. (2008) Stable isotope records of Late Quaternary climate and hydrology from Mediterranean lakes: the ISOMED synthesis. *Quaternary Sci Rev* 27:2426-2441

Rosenbaum J, Sheppard SMF. (1986) An isotopic study of siderites, dolomites and ankerites at high temperatures. *Geochim Cosmochim Acta* 50:1147-1150

Rosqvist GC, Leng MJ, Jonsson C. (2007) North Atlantic region atmospheric circulation dynamics inferred from a late-Holocene lacustrine carbonate isotope record, northern Swedish Lapland. *Holocene* 17:867-873

Roucoux KH, de Abreu L, Shackleton NJ, Tzedakis PC. (2005) The response of NW Iberian vegetation to North Atlantic climate oscillations during the last 65kyr. *Quaternary Sci Rev* 24:1637-1653

Ryves DB, Juggins S, Fritz SC, Battarbee RW. (2001) Experimental diatom dissolution and the quantification of microfossil preservation in sediments. *Palaeogeogr Palaeoclimatol* 172:99-113

Sánchez Goñi MF, Cacho I, Turon JL, Guiot J, Sierro FJ, Peypouquet JP, Grimalt JO, Shackleton NJ. (2002) Synchronicity between marine and terrestrial responses to millennial scale climatic variability during the last glacial period in the Mediterranean region. *Clim Dynam* 19:95-105

Schwander J, Eicher U, Ammann B. (2000) Oxygen isotopes of lake marl at Gerzensee and Leysin (Switzerland), covering the Younger Dryas and two minor oscillations, and their correlation to the GRIP ice core. *Palaeogeogr Palaeoclimatol* 159:203-214

Serra T, Soler M, Julia R, Casamitjana X, Colomer J. (2005) Behaviour and dynamics of a hydrothermal plume in Lake Banyoles, Catalonia, NE Spain. *Sedimentology* 52:795-808.

Sharp Z. (2007) *Principles of Stable Isotope Geochemistry*. Pearson Prentice Hall, New Jersey

Stoll HM, Moreno A, Mendez-Vicente A, Gonzalez-Lemos S, Jimenez-Sanchez M, Dominguez-Cuesta MJ, Edwards RL, Cheng H, Wang X. (2013) Paleoclimate and growth rates of speleothems in the northwestern Iberian Peninsula over the last two glacial cycles. *Quaternary Res* 80:284-290

Talbot MR. (1990) A review of the palaeohydrological interpretation of carbon and oxygen isotopic ratios in primary lacustrine carbonates. *Chem Geol* 80:261-279

Valero-Garcés B, Morellón M, Moreno A, Corella JP, Martín-Puertas C, Barreiro F, Pérez A, Giralt S, Mata-Campo MP. (2014) Lacustrine carbonates of Iberian Karst Lakes: Sources, processes and depositional environments. *Sediment Geol* 299:1-29

Valero-Garcés BL, González-Sampériz P, Navas A, Machín J, Delgado-Huertas A, Peña-Monné JL, Sancho-Marcén C, Stevenson T, Davis B. (2004) Paleohydrological fluctuations and steppe vegetation during the last glacial maximum in the central Ebro valley (NE Spain). *Quatern Int* 122:43-55

Valero-Garcés BL, Zeroual E, Kelts K. (1998) Arid Phases in the Western Mediterranean Region During the Last Glacial Cycle Reconstructed from Lacustrine Records. In: Benito G, Baker VR, Gregory KJ (eds), *Paleohydrology and Environmental Change*. John Wiley & Sons, London, pp 67-80

Vegas J, Ruiz-Zapata B, Ortiz JE, Galán L, Torres T, García-Cortés Á, Gil-García MJ, Pérez-González A, Gallardo-Millán JL. (2010) Identification of arid phases during the last 50 cal. ka BP from the Fuentillejo maar-lacustrine record (Campo de Calatrava Volcanic Field, Spain). *J Quaternary Sci* 25:1051-1062

Figure Captions

Fig. 1 Location of Lake Banyoles on the Iberian Peninsula (inset), and bathymetric map of the lake (modified from Moreno-Amich and García-Berthou 1989), showing the northern and southern sub-basins comprising several smaller karstic sinks. The drill site, BAN II (this study; 42°07'29"N, 2°45'29"E), and a previous core, La Draga, are located on the eastern margin of the lake. Based on a present-day digital elevation model from 5 m LIDAR data (CNIG; <http://centrodedescargas.cnig.es>) the possible lake extent has been simulated for a lake level rise of 3 m (white dashed line), which would make the terrestrial drill sites subaqueous. The city of Banyoles is located SE of the lake

Fig. 2 A) Atmospheric data from Banyoles, Catalonia, Spain (Banyoles Observatory 42°08'N, 02°45'E, 175 m a.s.l; average 2003-2013), including monthly precipitation amount (dark grey bars, P mm), temperature (average = solid line, range = light grey band; T °C) and humidity (dashed line; H %) (<http://www.meteobanyoles.com>). B) Isotope composition ($\delta^{18}\text{O}$ and δD) of long-term weighted mean annual rainfall (square) and monthly mean rainfall

(dots; inset: plotted by month) measured at Girona Airport (129 m a.s.l., 25 km south of Banyoles; IAEA-GNIP) between 2000 and 2006, corrected for altitude difference ($-0.6\%/100$ m; Fernández-Chacón et al. 2010), also shown are the Global Meteoric Water Line (GMWL; dashed line; Craig 1961) and the Western Mediterranean Meteoric Water Line (WMMWL; solid line; Celle-Jeanton et al. 2004)

Fig. 3 Multi-proxy data from core BAN II, including TIC, TOC, $\delta^{13}\text{C}_{\text{calcite}}$, $\delta^{18}\text{O}_{\text{calcite}}$. TIC, TOC and facies data were previously published (Höbig et al. 2012). The data fall into three main zones (3-1; roughly corresponding to MIS 3-1), which are marked. The data from BAN II are compared with those of a previous core (selected pollen taxa, Pérez-Obiol and Julià 1994; $\delta^{18}\text{O}_{\text{calcite}}$ and $\delta^{13}\text{C}_{\text{calcite}}$, Valero-Garcés et al. 1998), and corresponding horizons are indicated using dashed lines. Radiocarbon and U/Th ages are from Höbig et al. (2012) and cross-correlated from Valero-Garcés et al. (1998)

Fig. 4 Lake Banyoles summary percentage diatom diagram showing diatom zones DZ1-DZ6, defined using CONISS and the sum total of planktonic, facultative planktonic and benthic diatoms (% plankton is taken as an approximate indicator of lake level, although intervening samples devoid of diatoms may represent fluctuations not represented in the diatom data). The F-index ($\times 100$) is also indicated, ranging from 0 (all dissolving) to 100 (pristine)

Fig. 5 Revised age-depth model for core BAN II based on 8 calibrated AMS 14C dates, 3 U-series dates, and 1 tephra (Höbig et al. 2012), and 9 cross-correlated U-series dates from the La Draga core (Valero-Garcés et al. 1998). A 5 ka reservoir effect was applied to AMS 14C ages (after Morellón et al. 2014) and a 5.8 m-offset was assumed for cross-correlation

between the BAN II and La Draga cores based on the comparison of isotope data (see Fig. 3 and text for details)

Fig. 6 Monthly *d*-excess values calculated from isotope data measured at Girona Airport (IAEA-GNIP) between 2000 and 2006, showing the global average *d*-excess (+10‰, GMWL; Dansgaard 1964), and the western (+13.7‰, WMWL; Celle-Jeanton et al. 2001) and eastern (+20‰, EMWL; Dotsika et al. 2010) Mediterranean *d*-excess. Local monthly precipitation amount is shown (grey bars; P mm; <http://www.meteobanyoles.com>)

Fig. 7 Comparison of structural trends between Lake Banyoles BAN II $\delta^{18}\text{O}_{\text{calcite}}$ (plotted to depth with refined U-series chronological control as described in the text) and other North Atlantic and Mediterranean records (plotted to age). NGRIP ice core $\delta^{18}\text{O}_{\text{V-SMOW}}$ (NGRIP Members 2004), Portuguese margin MD95-2040 *Globigerina bulloides* $\delta^{18}\text{O}_{\text{V-PDB}}$ (de Abreu et al. 2003), Alborán Sea MD95-2043 *Globigerina bulloides* $\delta^{18}\text{O}_{\text{V-PDB}}$ (Cacho et al. 1999), Ionian Sea M25/4-11 *Globigerinoides ruber* (solid line) and *Globigerina bulloides* (dashed line) $\delta^{18}\text{O}_{\text{V-PDB}}$ (Allen et al. 1999) and Soreq Cave, Israel speleothem $\delta^{18}\text{O}_{\text{V-PDB}}$ (Bar-Matthews et al. 1999). Grey bars indicate the INTIMATE event stratigraphy (Blockley et al. 2012) and dashed lines demarcate MIS 3-1

Fig. 1

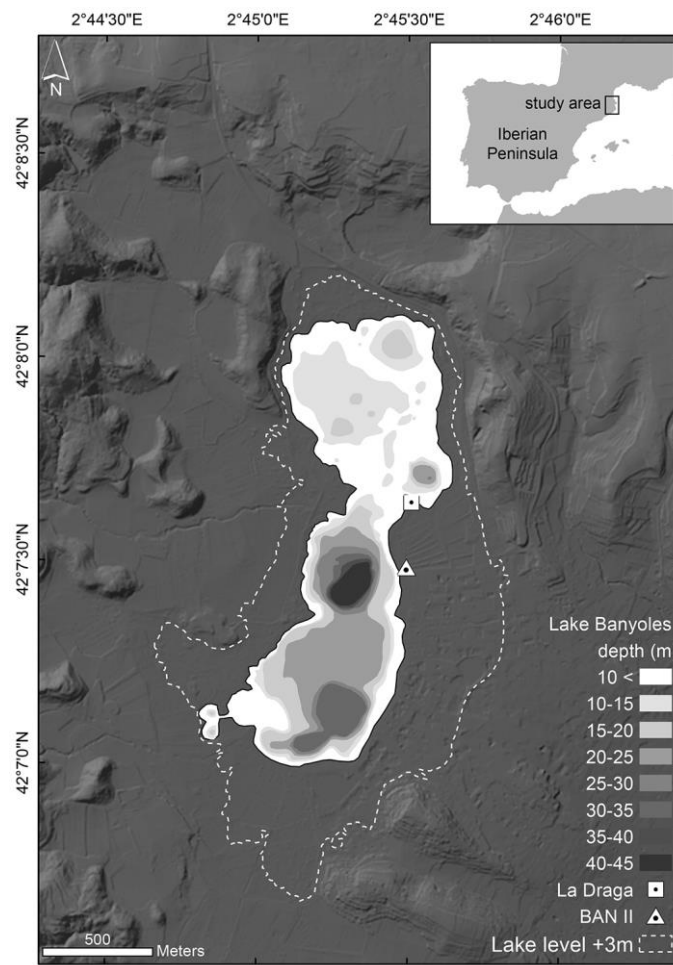


Fig. 2

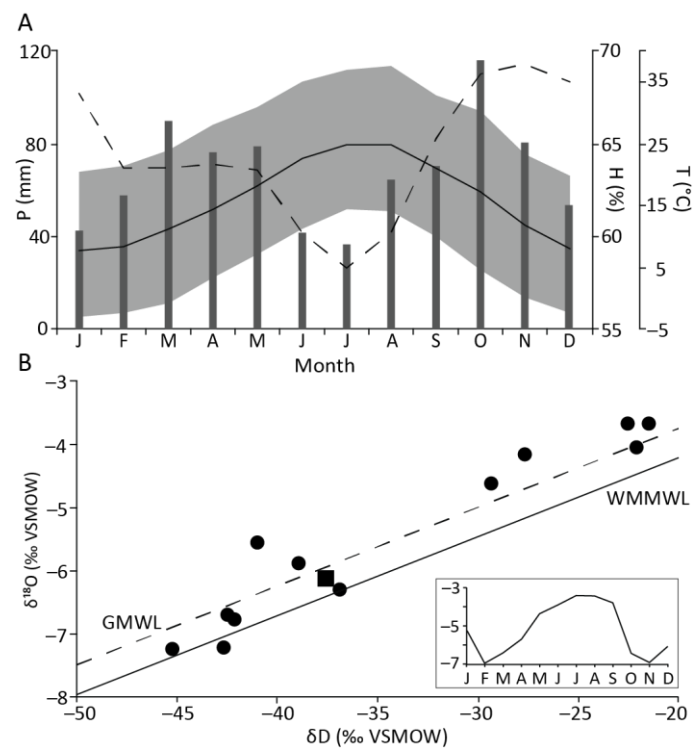


Fig. 5

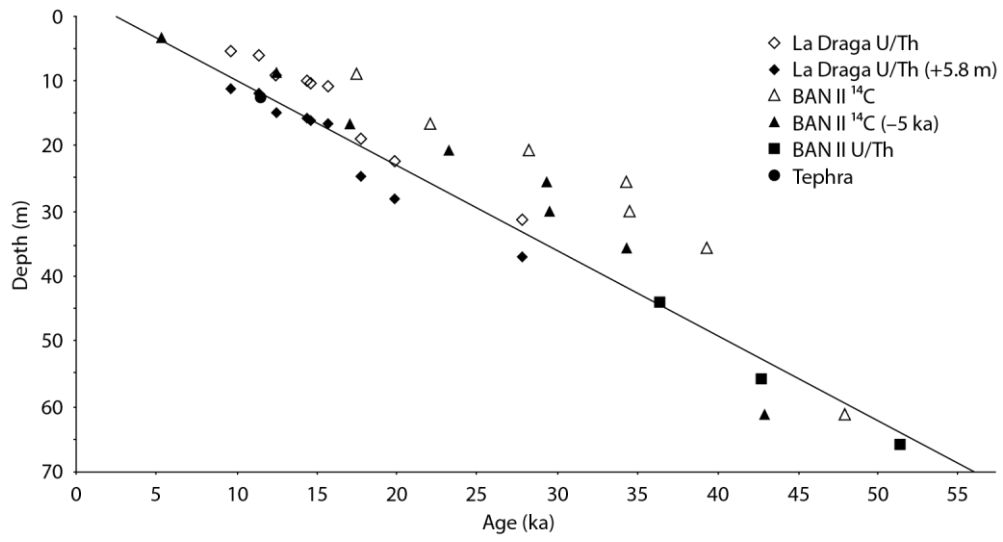


Fig. 6

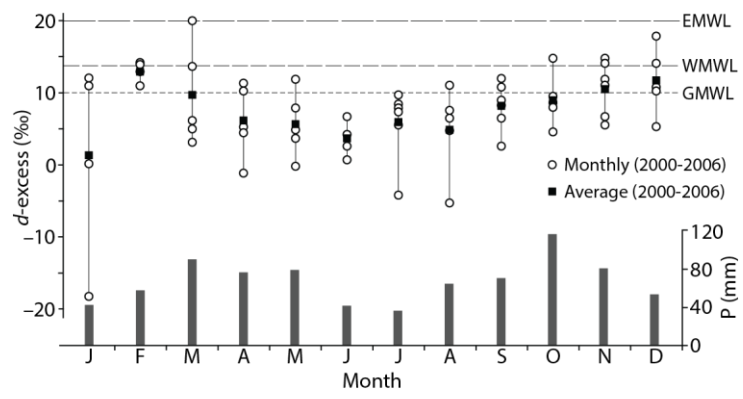


Fig. 7

